

EFFECT OF SINTERING ON SOME PROPERTIES OF NiZn-FERRITE

A THESIS SUBMITTED IN PARTIAL FULLFILLMENT OF THE REQUIREMENTS FOR
THE DEGREE OF BACHELOR OF TECHNOLOGY

By

DEBAJYOTI MOHANTY

Roll No: 107CR011



DEPARTMENT OF CERAMIC ENGINEERING

NATIONAL INSTITUTE OF TECHNOLOGY

ROURKELA

2010-2011

EFFECT OF SINTERING ON SOME PROPERTIES OF NiZn-FERRITE

A THESIS SUBMITTED IN PARTIAL FULLFILLMENT OF THE REQUIREMENTS FOR
THE DEGREE OF BACHELOR OF TECHNOLOGY

By

DEBAJYOTI MOHANTY

Roll No: 107CR011

Under the Guidance of

Prof. JAPES BERA



DEPARTMENT OF CERAMIC ENGINEERING

NATIONAL INSTITUTE OF TECHNOLOGY

ROURKELA

2010-2011



**NATIONAL INSTITUTE OF TECHNOLOGY
ROURKELA 2011**

CERTIFICATE

This is to certify that the thesis entitled, **“EFFECT OF SINTERING ON SOME PROPERTIES OF NiZn-FERRITE”** submitted by **Mr. Debajyoti Mohanty** in partial fulfillment of the requirements of the award of Bachelor of Technology Degree in Ceramic Engineering at the National Institute of Technology, Rourkela is an authentic work carried out by him under my supervision and guidance.

To the best of my knowledge, the matter embodied in the thesis has not been submitted to any other university / institute for the award of any Degree or Diploma.

Prof. Japes Bera
Dept. of Ceramic Engineering
National Institute of Technology
Rourkela – 769008

Date: 11.5.2011

ACKNOWLEDGEMENTS

With deep regards and profound respect, I avail this opportunity to express my deep sense of gratitude and indebtedness to Prof. Japes Bera, Head, Department of Ceramic Engineering, N I T Rourkela for providing me the present topic and for his superb guidance, and all the invaluable suggestions. I thank him for all the constructive feedbacks provided by him during my work. Whenever I did the analysis wrong, he always remained calm and guided me to the correct path and always supported me as the best mentor. I am grateful to him.

I would also like to thank all the other professors including Prof. Maity, Prof. S. K. Pratihari, Prof. S. Bhattacharya, Prof. D. Sarkar, Prof. S. Pal, Prof. B. B. Nayak, Prof. R. Sarkar, Prof. R. Majumdar and Prof. A. Chowdhury for their valuable suggestions during the research work.

I would also like to thank all the PhD and MTech scholars especially Geetanjali and Bhabanibhai for helping me out of difficult situations whenever I asked for help.

I am grateful to Prof. Pawan Kumar, Department of Physics for providing me the necessary equipment needed for magnetic testing of my samples. I would like to thank the PhD scholar Prakashbhai, Department of Physics for helping in the magnetic testing.

The staff members of the Department of Ceramic Engineering were very helpful during the research work and I would like to thank them for that.

And at last but not the least, my thanks and love to all my buddies who always stood up to me and shone like the light at the end of a tunnel.

11th May 2011

Debajyoti Mohanty

Abstract

The present investigation reports effect of densification on the magnetic properties (initial permeability and relative loss factor) of Ni-Zn ferrites with a composition $(\text{Ni}_{0.68}\text{Zn}_{0.25}\text{Mn}_{0.02})\text{Fe}_{2.5}\text{O}_4$.

NiZn-ferrite toroid samples of the above composition, supplied by one industry, were sintered at three temperatures; 1000°C, 1050°C and 1100°C and for three different periods of 15 mins, 1 hr and 4 hrs. The X-ray diffraction pattern confirms the formation of cubic spinel phase.

In the above samples, the highest densification achieved was 84.71 % (of theoretical density) at 1100°C 4hrs. The sintering temperature was kept low to minimize the ZnO evaporation loss.

Magnetic measurements were performed at 100 KHz (0.01 V) using a LCR meter and showed a maximum inductance of 3.9501 μH . The highest initial permeability was 67.83 and the relative loss factor varied from 0.0143 to 0.00178 i.e. in between the range 10^{-2} to 10^{-3} .

Also, the dependency of permeability and loss were measured in the range of 42 Hz to 1 MHz. A decrease in initial permeability was observed with increasing frequency. Better magnetic properties (at high frequencies) have been noted in the samples with higher densities.

CONTENTS

	Page no.
<i>Acknowledgements</i>	4
<i>Abstract</i>	5
<i>Table of Contents</i>	6
<i>List of Figures</i>	7
<i>List of Tables</i>	8
CHAPTER-1 Introduction	9
CHAPTER-2 Literature Review	12
CHAPTER-3 Experimental Work	16
3.1 Densification measurement	16
3.2 Magnetic measurement	18
CHAPTER-4 Results and Discussion	19
4.1 Densification characterization	19
4.2 Magnetic characterization	23
4.2.1 Initial Permeability	23
4.2.2 Loss	27
CHAPTER-5 Conclusions	31
References	32

LIST OF FIGURES

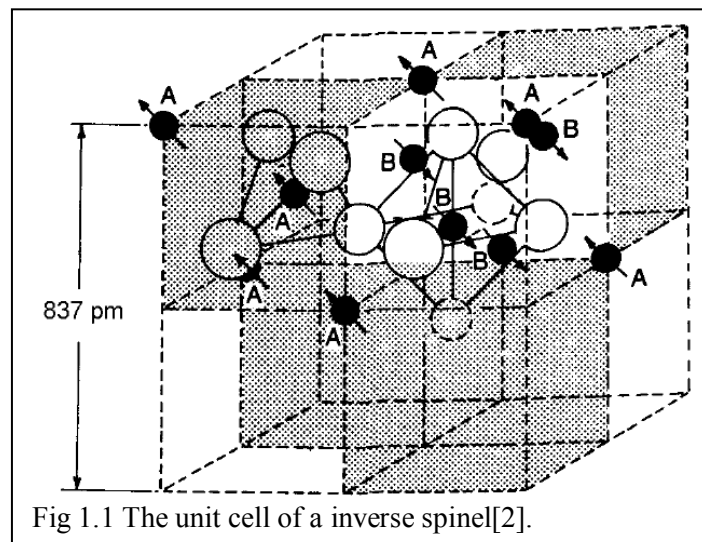
S. no.	Figure nos.	Title of Figure	Page no.
1	Fig. 1.1	Unit cell of a magnetic inverse spinel	9
2	Fig. 1.2	Saturation magnetization per formula unit of the ferrite $(Fe_{1-\delta}^{3+}Zn_{\delta}^{2+})(Fe_{1+\delta}^{3+}Ni_{1-\delta}^{2+})O_4$ as a function of δ	11
3	Fig 2.1	Variation of permeability as a function of frequency for the ferrites sintered at 1150, 1250 and 1350 °C	13
4	Fig. 2.2	Variation of relative loss factor as a function of frequency for the ferrites sintered at 1150, 1250 and 1350 °C	13
5	Fig. 2.3	Frequency variation of μ_i' of $Ni_{1-x}Zn_xFe_2O_4$ sintered at 1200 and 1400°C	14
6	Fig. 2.4	Frequency variation of μ_i'' of $Ni_{1-x}Zn_xFe_2O_4$ sintered at 1200 and 1400°C	15
7	Fig. 3.1	Schematic of a toroid core	16
8	Fig. 4.1	XRD pattern of the ferrite.	19
9	Fig. 4.2	Theoretical Density(d/d_{th}) v/s Sintering Time for three sintering temperatures, 1000°C, 1050°C and 1100°C	20
10	Fig. 4.3	Theoretical Density(d/d_{th}) v/s Sintering Temperature for three sintering times, 15 mins, 1 hr and 4 hrs.	21
11	Fig. 4.4	Microstructure and EDS spectra of sintered ferrite	22
12	Fig. 4.5	μ_i v/s sintering time at fixed frequency 100 KHz	23
13	Fig. 4.6	μ_i v/s Frequency for samples sintered at 1000°C	24
14	Fig. 4.7	μ_i v/s Frequency for samples sintered at 1050°C	24
15	Fig. 4.8	μ_i v/s Frequency for samples sintered at 1100°C	25
16	Fig. 4.9	μ_i v/s Frequency for samples sintered for 15 mins	25
17	Fig. 4.10	μ_i v/s Frequency for samples sintered for 1 hr	26
18	Fig. 4.11	μ_i v/s Frequency for samples sintered for 4 hrs	26
19	Fig. 4.12	RLF($\tan\delta/\mu_i$) v/s Frequency for samples sintered at 1000°C	27
20	Fig. 4.13	RLF($\tan\delta/\mu_i$) v/s Frequency for samples sintered at 1050°C	28
21	Fig. 4.14	RLF($\tan\delta/\mu_i$) v/s Frequency for samples sintered at 1100°C	28
22	Fig. 4.15	RLF($\tan\delta/\mu_i$) v/s Frequency for samples sintered for 15 mins	29
23	Fig. 4.16	RLF($\tan\delta/\mu_i$) v/s Frequency for samples sintered for 1 hr	29
24	Fig. 4.17	RLF($\tan\delta/\mu_i$) v/s Frequency for samples sintered for 4 hrs	30
25	Fig. 4.18	RLF($\times 10^{-3}$) vs. %Theoretical density at 100 KHz fixed frequency	30

LIST OF TABLES

S. no.	Table nos.	Title of Table	Page no.
1	Table 3.1	Densification Characteristics	20
2	Table 4.1	Peak List, d-spacing[Å], (h k l) plane and lattice parameter (a in Å)	21

NiZn ferrite is a spinel ferrite. Magnetic spinels have the general formula $MO \cdot Fe_2O_3$ or MFe_2O_4 where, M is divalent metal ionlike Mn, Zn, Ni, Fe, or Co (or a mixture of such ions)[1].

In the spinel crystal structure the oxygen ions form a cubic close-packed array in which two types of interstice occur, one coordinated tetrahedrally and the other octahedrally with oxygen ions. The cubic unit cell is large, comprising eight formula units and containing 64 tetrahedral and 32 octahedral sites, customarily designated A and B sites respectively; eight of the A sites and 16 of the B sites are occupied. The unit cell shown in Fig. 1.1 is seen to be made up of octants, four containing one type of structure (shaded) and four containing another (unshaded). In this representation some of the A-site cations lie at the corners and face-centre positions of the large cube; a tetrahedral and an octahedral site are shown. The close-packed layers of the oxygen ion lattice lie at right angles to the body diagonals of the cube. The arrows on the ions, representing directions of magnetic moments, indicate that the B-site ions have their moments directed antiparallel to those of A-site ions, illustrating the antiferromagnetic coupling[2].



In a spinel structure, both divalent and trivalent cations are distributed among tetrahedral (A) and octahedral (B) sites. The site preference exhibited by divalent ions defines whether the spinel is normal, inverse or mixed.

In normal spinel, the A^{2+} ions occupy only tetrahedral sites and the B^{3+} ions occupy only octahedral sites, for eg. $ZnFe_2O_4$.

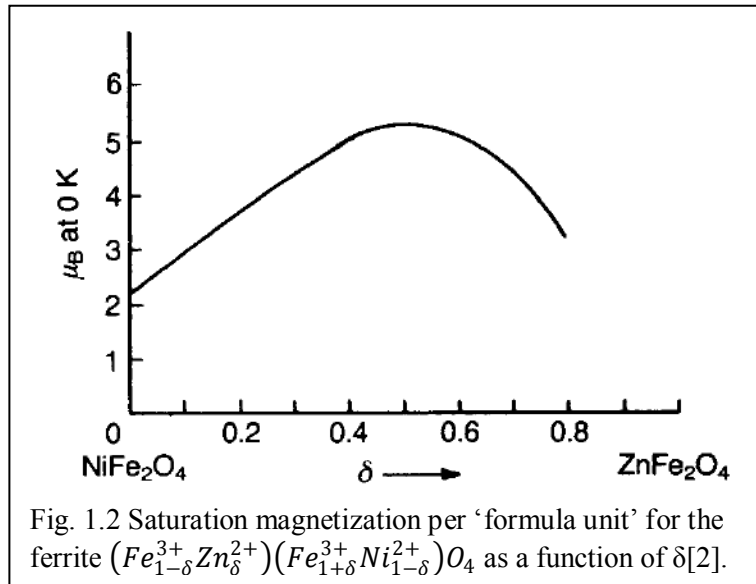
In inverse spinel, all the A^{2+} ions and half the B^{3+} ions sit on the octahedral sites; the tetrahedral sites are occupied now by the other half of the B^{3+} ions, for eg. $NiFe_2O_4$.

In most cases, magnetic divalent cations (such as Ni^{2+}) prefer the octahedral sites and produce an inverse spinel structure. Diamagnetic divalent cations (such as Zn^{2+} , Cd^{2+}) have preference for the tetrahedral positions and the resulting structure is a normal spinel [3].

Therefore, NiZn ferrite shows a mixed spinel structure.

Addition of a non-magnetic ion such as Zn to a spinel ferrite leads to an increase in saturation magnetization. The magnetic moment per formula unit MFe_2O_4 , where M represents Ni^{2+} or Zn^{2+} , is shown in Fig. 1.2 as a function of zinc substitution. Zinc ferrite is a normal spinel, indicating that Zn ions have a preference for the A sites, so that on substituting zinc for nickel the occupancy becomes $(Fe_{1-\delta}^{3+}Zn_{\delta}^{2+})(Fe_{1+\delta}^{3+}Ni_{1-\delta}^{2+})O_4$ in which the first and second brackets indicate occupancy of the A and B sublattices respectively. Thus the antiparallel coupling between moments on A and B sites is reduced because the occupancy of A sites by magnetic ions is reduced, and as a consequence the Curie point is lowered. However, the excess of moments on octahedral sites over those on tetrahedral sites is increased so that the magnetization is increased. The data plotted in Fig. 1.2 confirm this model up to $\delta \sim 0.4$. The fall in

magnetization for higher values of δ is due to the reduced antiparallel coupling between the A and B sites, and it becomes zero when $\delta=1$, i.e. $(Zn^{2+})(Fe_2^{3+})O_4$



Generally speaking, the spinel ferrites have low magnetic anisotropies and are magnetically 'soft'; exceptions are those containing Co^{2+} which is itself strongly magnetically anisotropic. Cobalt spinel ferrites can have coercivities approaching $10^5 Am^{-1}$, placing them firmly in the 'hard' category[2].

Ni-Zn ferrites are one of the most versatile magnetic materials for general use, which have many applications in both low and high frequency devices and play a useful role in many technological applications such as microwave devices, rod antennas, read/write heads for high speed digital tape, cores for inductors, transformers and in switch mode power supplies etc. because of their high initial permeability, low magnetic losses, high resistivity, low dielectric losses, mechanical hardness, high Curie temperature and chemical stability[4,5].

Nickel–zinc ferrites have excellent soft magnetic properties and are used in electronic and telecommunication industries. Ferrites are structure sensitive materials and their properties critically depend on the manufacturing process [6].

The densification of a pure NiZn ferrite to a reasonably high density is difficult because of the relatively high melting point of some component oxides and low bulk diffusivity. As a result, it is very difficult to obtain a sintered body with density exceeding 90% of the theoretical density using solid state sintering. At the same time, typical NiZn ferrites sinter satisfactorily only above 1250 °C, their microstructure and properties being difficult to control because of the volatility of ZnO at such temperatures[7].

The magnetic properties of ferrites are known to be influenced by chemical composition, crystal structure, grain size and porosity. Initial permeability is an important magnetic property to study the quality of soft ferrites [6].

R. V.Mangalaraja et al. [6] reported the initial permeability(μ_i) and the relative loss factor ($\tan \delta/\mu_i$) as the function of frequency in the range of 1 kHz to 13 MHz for $\text{Ni}_{0.8}\text{Zn}_{0.2}\text{Fe}_2\text{O}_4$ prepared by the flash combustion technique and sintered at 1150, 1250 and 1350 °C which shows a steep fall up to 10 kHz as shown in fig.2.1. Thereafter, no variation is seen for these samples up to 6MHz. At 6 MHz, the trend slightly changes and the permeability value for all the samples slowly increases up to 13 MHz. The initial permeability value lies between 18 and 23. The sample sintered at 1350 °C shows a permeability value of ≈ 23 . The same order of values was obtained by *Verma et al.*[8] for the ferrite. The increase in the sintering temperature results in a decrease in the magnetic anisotropy by decreasing the internal stress and crystal anisotropy, which reduce the

hindrance to the movement of the domain walls resulting thereby in the increased value of the initial permeability[8].

The relative loss factor ($\tan \delta/\mu_i$) is shown in Fig. 2.2 for Ni-Zn ferrites sintered at various temperatures[6].

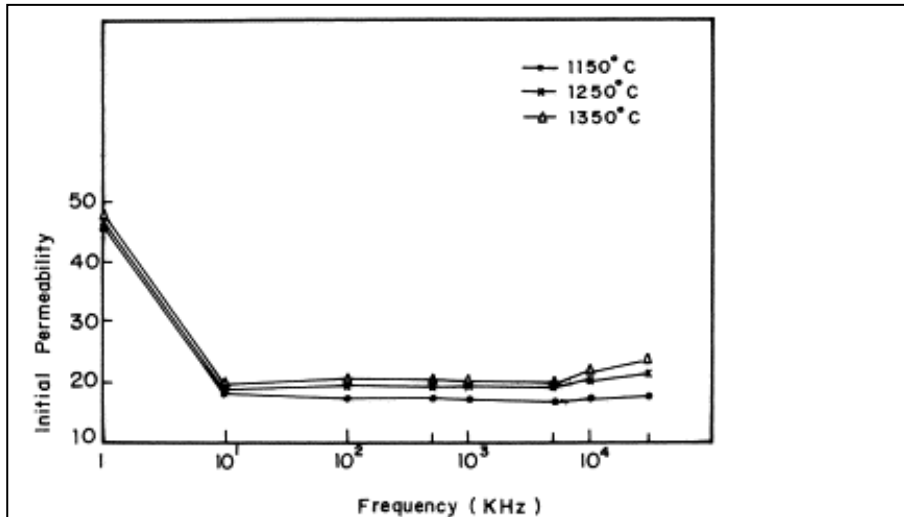


Fig 2.1 Variation of permeability as a function of frequency for the ferrites sintered at 1150, 1250 and 1350 °C [6].

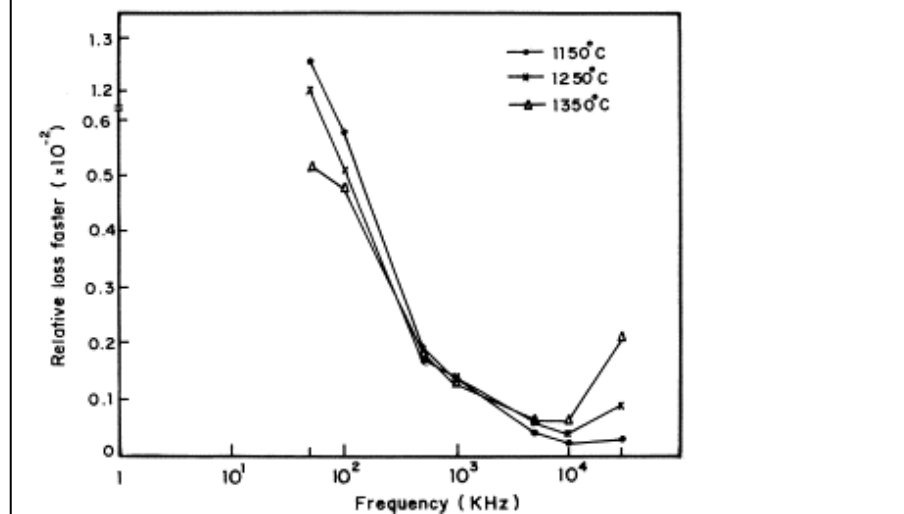


Fig 2.2 Variation of relative loss factor as a function of frequency for the ferrites sintered at 1150, 1250 and 1350 °C [6].

Verma *et al.* [8] reported the initial permeability (μ_i) and the relative loss factor ($\tan \delta/\mu_i$) as the function of frequency in the range of 10 KHz–13 MHz for samples of composition $\text{Ni}_{1-x}\text{Zn}_x\text{Fe}_2\text{O}_4$, with $x=0.2, 0.35, 0.5$ and 0.6 sintered in the range $1100\text{--}1400^\circ\text{C}$ for 1 h in air. The variations of the real part μ_i' and of the imaginary part μ_i'' of complex initial permeability with frequency are studied as a function of the composition and sintering temperature. Typical variations of all the compositions sintered at 1200 and 1400°C are shown in Fig. 2.3 and Fig. 2.4, respectively. The variation in μ_i' and μ_i'' as a function of frequency for $\text{Ni}_{1-x}\text{Zn}_x\text{Fe}_2\text{O}_4$ samples sintered at four different temperatures ($1100, 1200, 1300$ and 1400°C) showed similar behaviour. μ_i' and μ_i'' are observed to vary both with sintering temperature and zinc content.

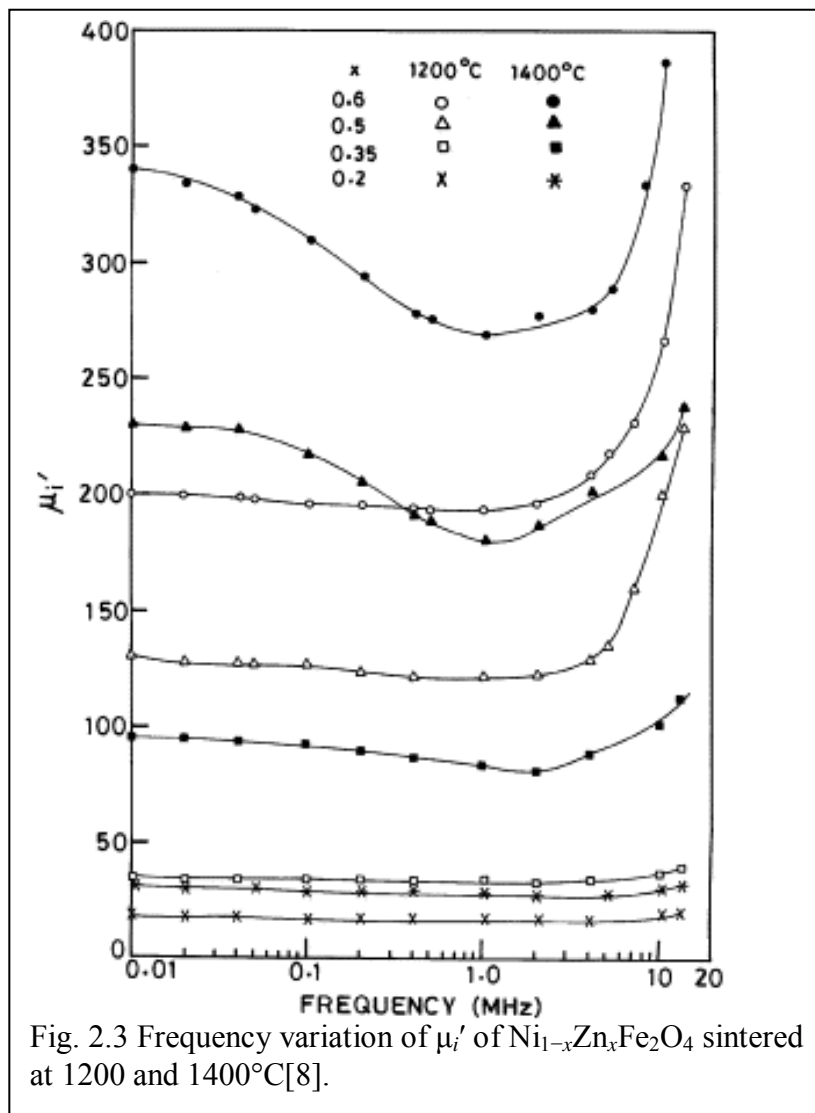
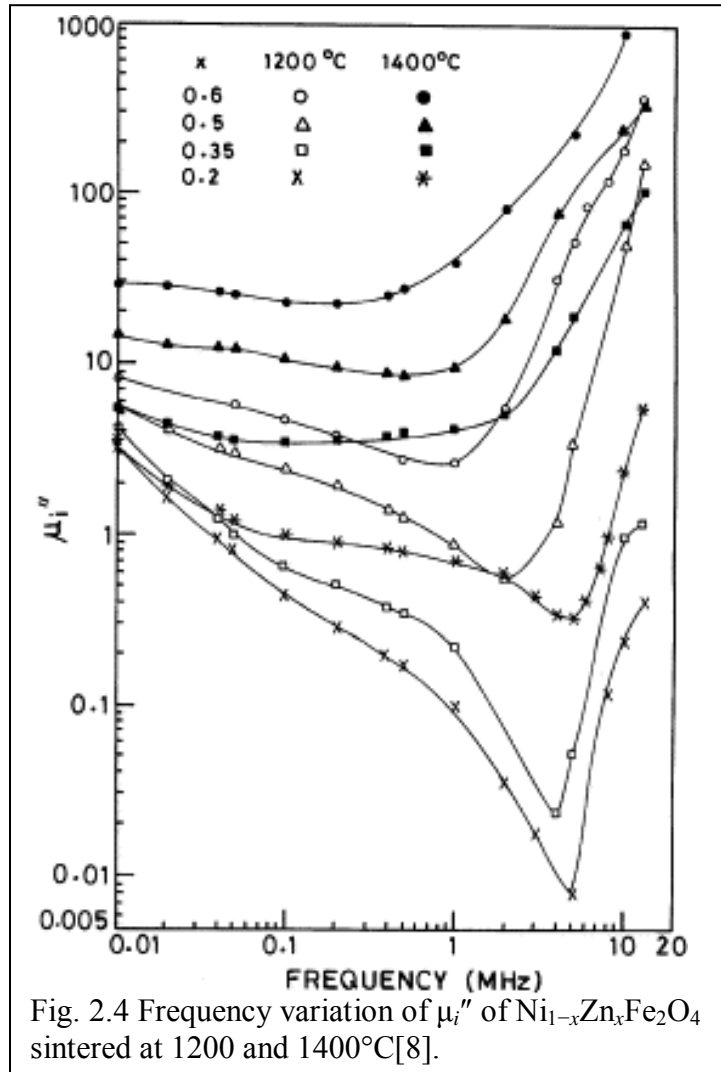


Fig. 2.3 Frequency variation of μ_i' of $\text{Ni}_{1-x}\text{Zn}_x\text{Fe}_2\text{O}_4$ sintered at 1200 and 1400°C [8].



OBJECTIVE

The objective of present study is to investigate the influence of sintering temperature and time on densification, initial permeability, loss factor of commercially utilized NiZn Ferrite toroidal core.

Ring core made of NiZn-Ferrite with a typical industrial composition of $(\text{Ni}_{0.68}\text{Zn}_{0.25}\text{Mn}_{0.02})\text{Fe}_{2.5}\text{O}_4$ has been used for the study of effect of sintering temperature and time on the properties of the ferrite. The green toroid core had the dimensions of approximately 30 mm outer diameter, 17 mm inner diameter and 17 mm height as per the following diagram:

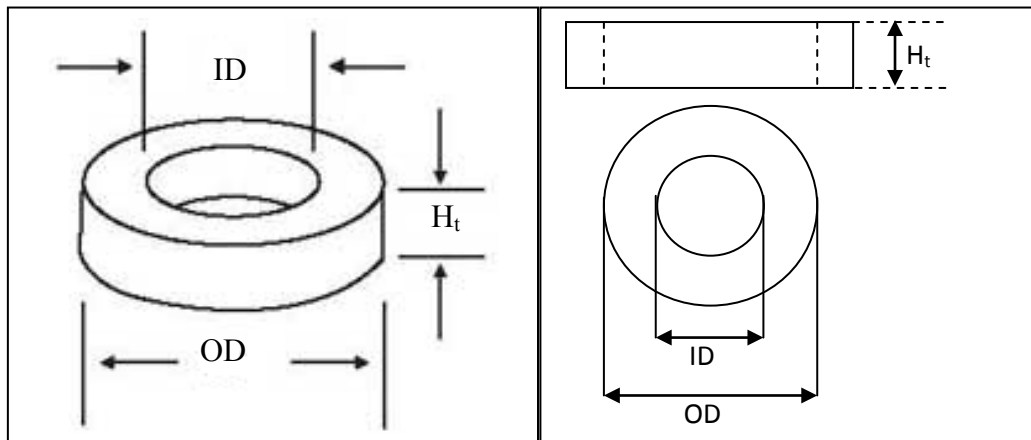


Fig. 3.1 Schematic of the toroid core

3.1 Densification measurement

The green densities of the cores were measured from geometrical dimension and weight of the specimens. The average green density was 3.03 g/cc. The green densities of individual specimens are shown in table 3.1 below.

The specimens were sintered at three different temperatures of 1000, 1050 and 1100°C for three different times of 15, 60 and 240 minutes respectively at peak temperature. The temperature and time of sintering are also shown in table 3.1. During sintering

experiment, a heating rate of 10°C/min was maintained to evaporate small amount of binders from the green specimen.

The sintered densities of each specimen were also measured (shown in table 3.1) from geometrical dimensions and weight of them.

To measure the theoretical density of the ferrite, one sintered specimen was powdered and powder X-Ray Diffraction analysis was done using Philips XRD (Model: PW 1830 diffractometer, Netherland) in 2θ range 15-60°.

From the diffraction pattern, the lattice parameter of the ferrite was determined using formula:

$$a = d\sqrt{(h^2 + k^2 + l^2)}$$

(For cubic system)

X-Ray density was calculated using the formula:

$$D = \frac{FW \times Z \times 1.66}{V}$$

Where,

D = X-Ray Density or Theoretical Density(g/cc)

FW = Formula wt. of the spinel(a.m.u)

Z = No. of formula units per unit cell

V = Volume of the unit cell(Å³)

1.66 is the multiplication factor for the unit conversion.

Sintered densities were then converted to % Theoretical density using this X-Ray density.

3.2 Magnetic measurement

For magnetic measurement, the toroid samples were wound with 6 turns of low capacitive winding. The inductance and $\tan\delta$ of the toroidal core were measured using Hyoki Low Frequency LCR meter(Japan), in the frequency range 42 Hz to 1 MHz.

Initial permeability of the core was calculated using the formula:

$$\mu_i = \frac{L}{2 \times 10^{-7} \times N^2 \times H_t \times \ln\left(\frac{OD}{ID}\right)}$$

Where,

L = Inductance

N =No. of turns

H_t =Height of the core

OD =Outer diameter of the core

ID =Inner diameter of the core

2×10^{-7} =Conversion factor

The relative loss factor i.e $\tan\delta/\mu_i$ were calculated for each core.

4.1 Densification Characterization

Fig. 4.1 shows the XRD pattern of the ferrite. The pattern matched with the standard NiZn ferrite with reference code 08-0234 from the standard pattern respective h,k,l values of the diffraction peaks were assigned. They are represented in Table 4.1 along with the peak position 2θ , d-spacing (in Å). The a-value calculated as per the eq. stated in the previous chapter for each peak and is also mentioned in the Table 4.1. The average a-value for the material was 8.3757 Å. Using this a-value, theoretical density was found out to be 5.33 g/cc.

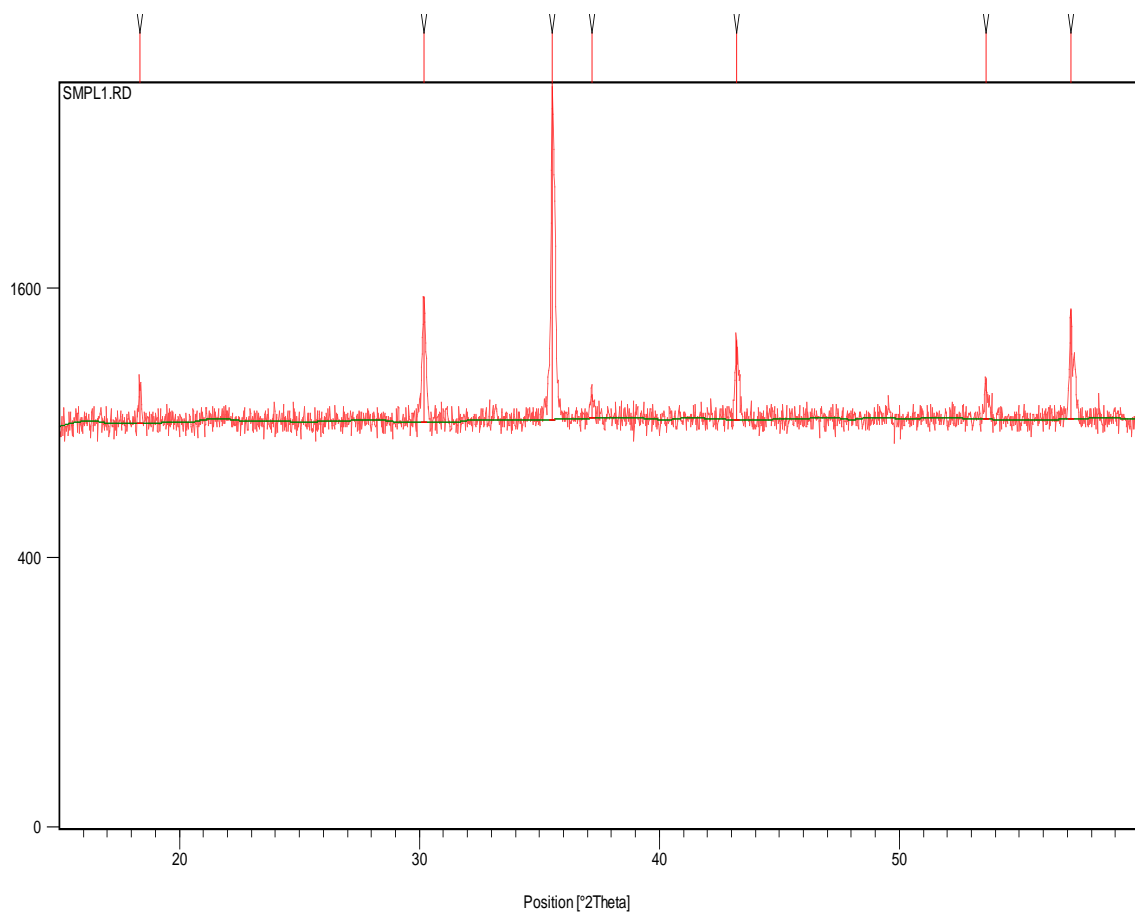


Fig. 4.1 XRD pattern of the ferrite.

Table 4.1 Peak List, d-spacing[Å], (h k l) plane and lattice parameter (a in Å).

Pos.[°2Th.]	d-spacing[Å]	(h k l) plane	a-value
18.3473	4.83566	(111)	8.3756
30.1865	2.96069	(220)	8.3741
35.5403	2.52601	(311)	8.3778
37.1875	2.41782	(222)	8.3756
43.2110	2.09372	(400)	8.3749
53.6015	1.70981	(422)	8.3763
57.1463	1.61056	(511)	8.3687
Average a-value:			8.3757

Fig. 4.2 shows the % densification (of theoretical density) with sintering time for three different sintering temperatures. The green density, bulk density and % th. Densities are also shown in the Table 4.2. The figure shows the % densification with sintering temperature for three different sintering times. As expected, densification increases with increasing sintering temperature as well as time. % Theoretical density v/s Sintering Temperature for three sintering times, 15 mins, 1 hr and 4 hrs are also shown in Fig. 4.3 showing similar behavior of increased density with time.

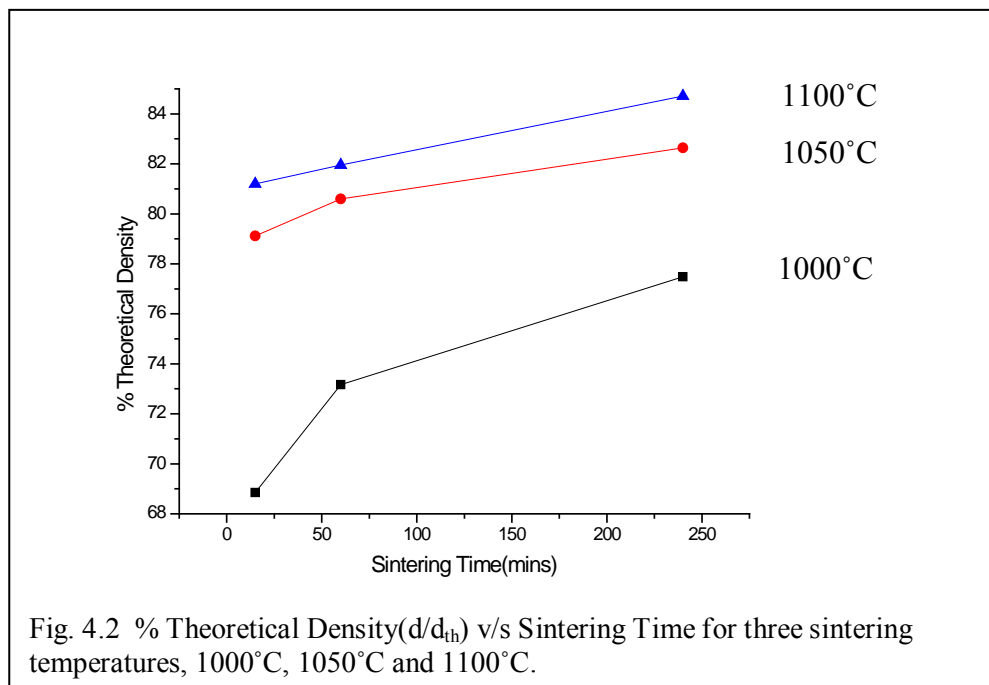
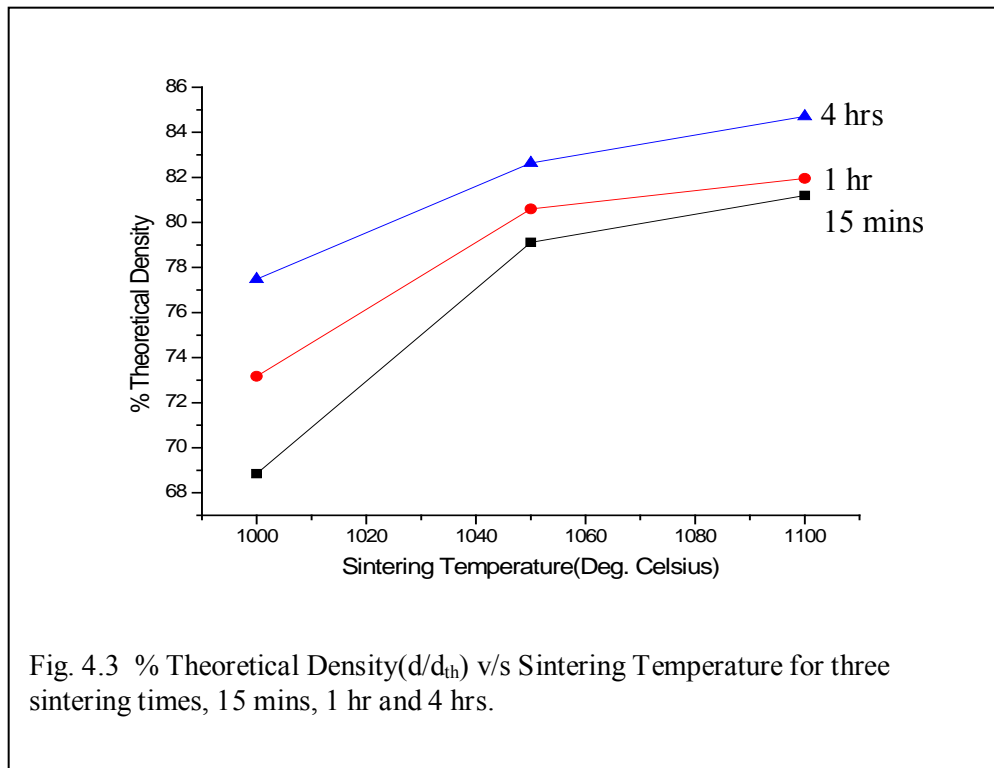


Table 4.2 Densification Characteristics

Sintering Temperature(°C)	Sintering Time(mins)	Green Density(g/cc)	Density After Firing(g/cc)	% Densification	% Theoretical Density
1000°C	15	3	3.67	18.26	68.85
1000°C	60	3.06	3.89	21.34	73.17
1000°C	240	3.05	4.13	26.15	77.48
1050°C	15	3.06	4.22	27.49	79.12
1050°C	60	3.05	4.3	29.07	80.6
1050°C	240	3.02	4.41	31.52	82.64
1100°C	15	3.04	4.33	29.79	81.2
1100°C	60	3.05	4.37	30.21	81.95
1100°C	240	3.02	4.52	33.19	84.71



Sintered ferrite microstructure is shown in Fig. 4.4 along with its EDS spectra. The micrograph for 1000°C sintered specimen shows a average 1 micron grains of the ferrite with lot of open porocities. The EDS spectra show the presence of Ni, Zn and Fe are the major constituents.

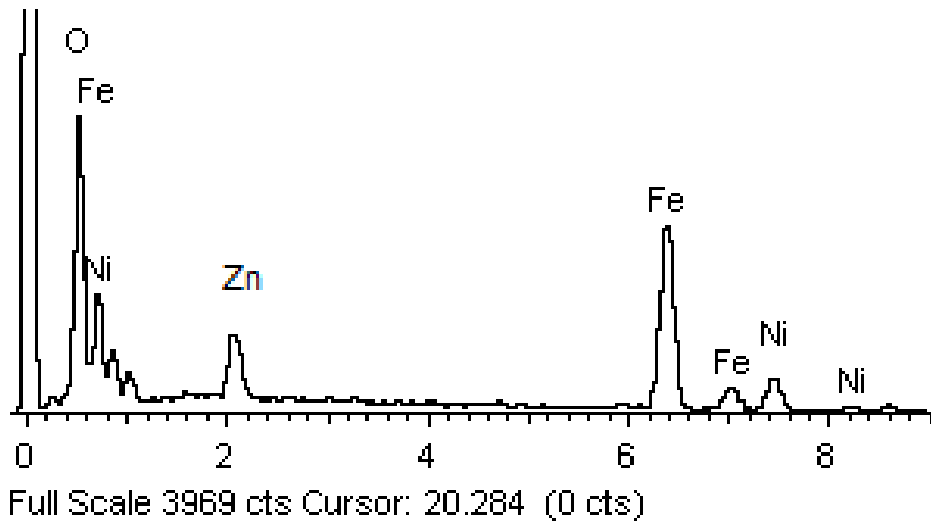
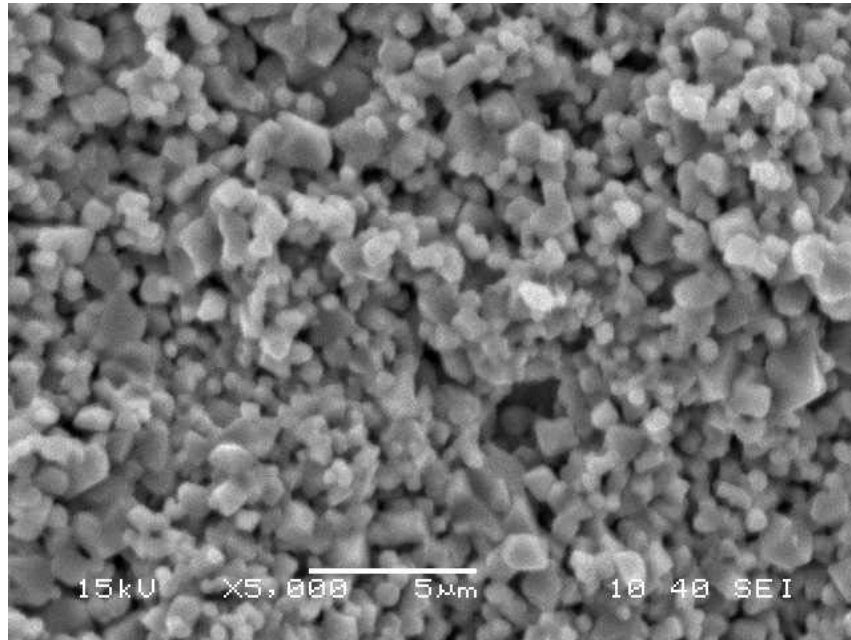


Fig. 4.4 Microstructure and EDS spectra of sintered ferrite.

4.2 Magnetic Characterization

4.2.1 Initial Permeability(μ_i)

Fig. 4.5 shows the initial permeability v/s sintering time and temperature at 100 kHz frequency.

Permeability increases with increase in sintering temperature. This is due to a decrease in the magnetic anisotropy by decreasing the internal stress and crystal anisotropy, which reduces the hindrance to the movement of the domain walls resulting thereby in the increased value of the initial permeability[8].

Permeability increases with the increase in density which may be due to an increase in the contribution from domain wall displacement.

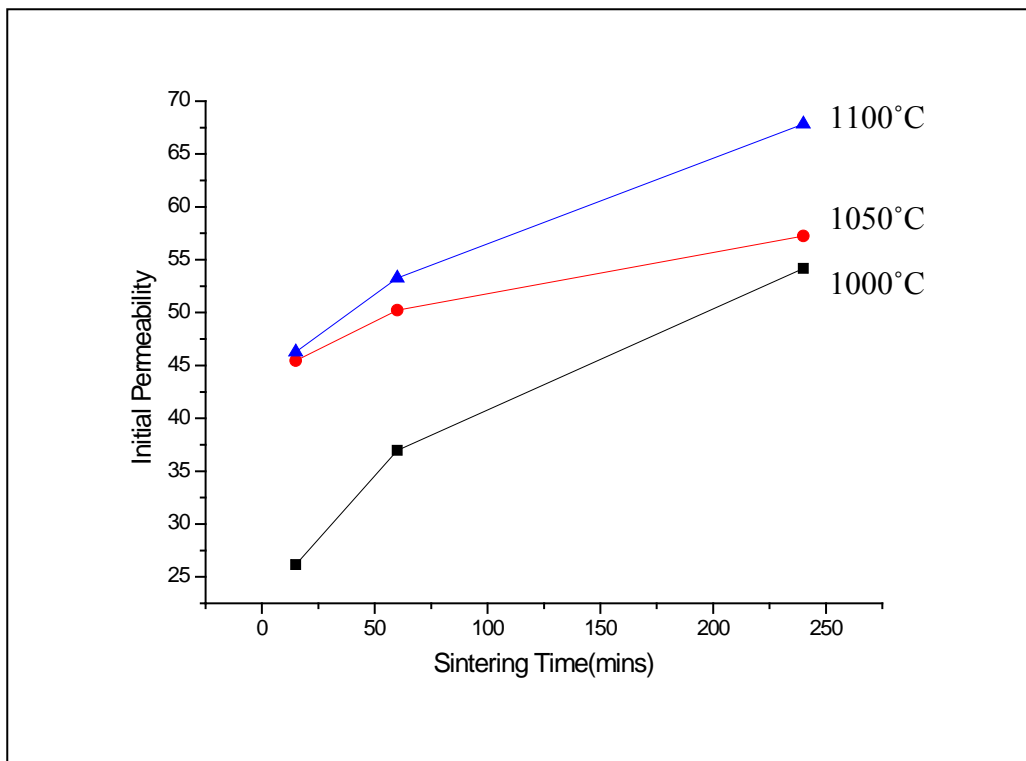
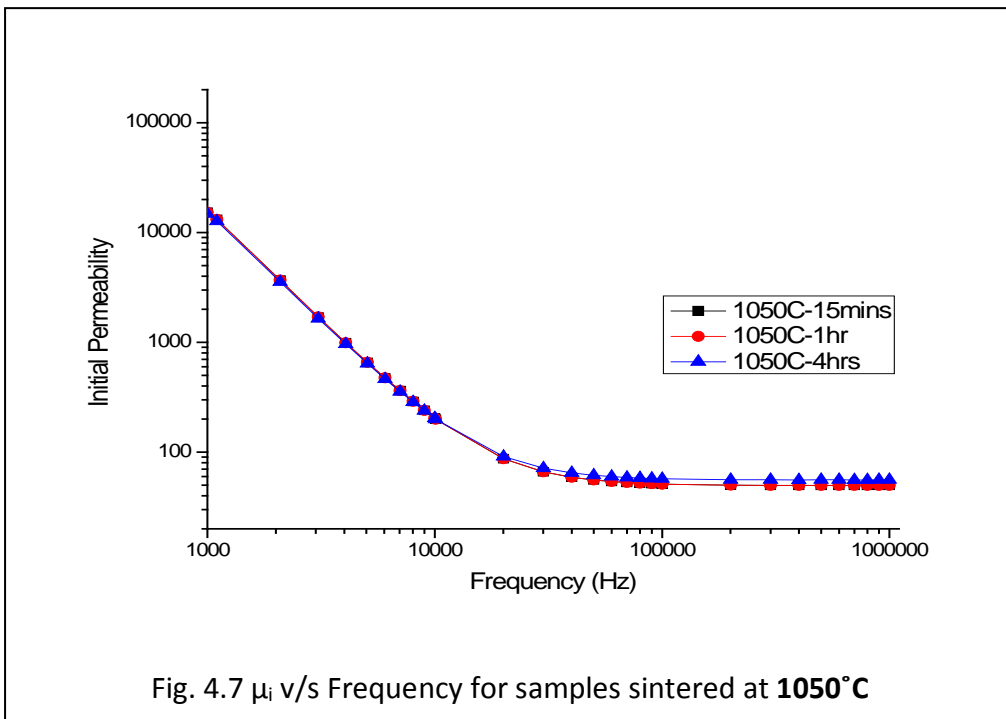
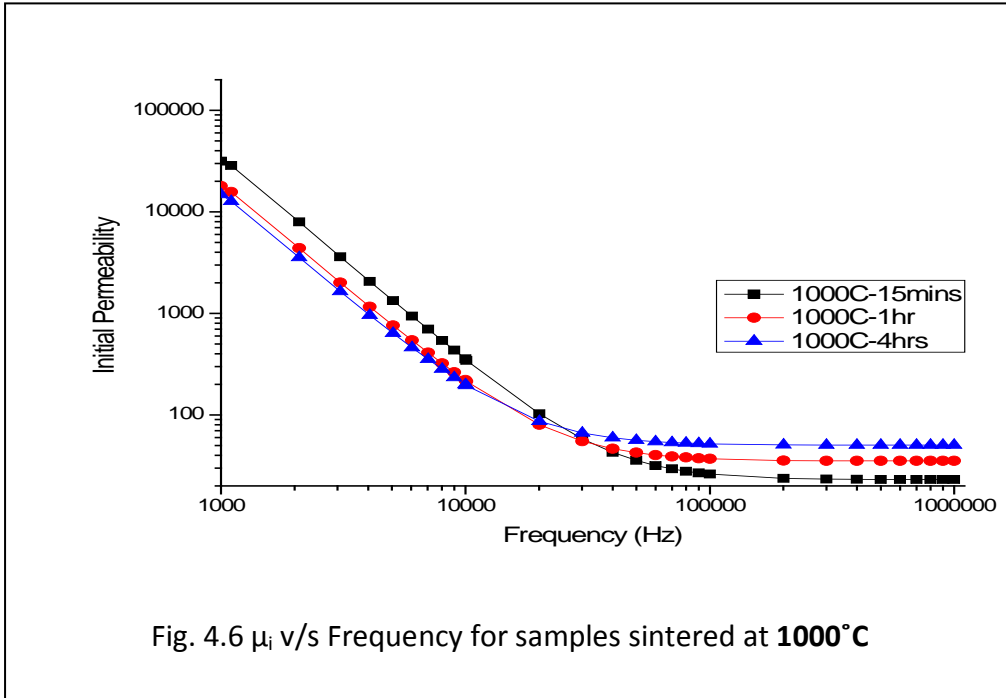
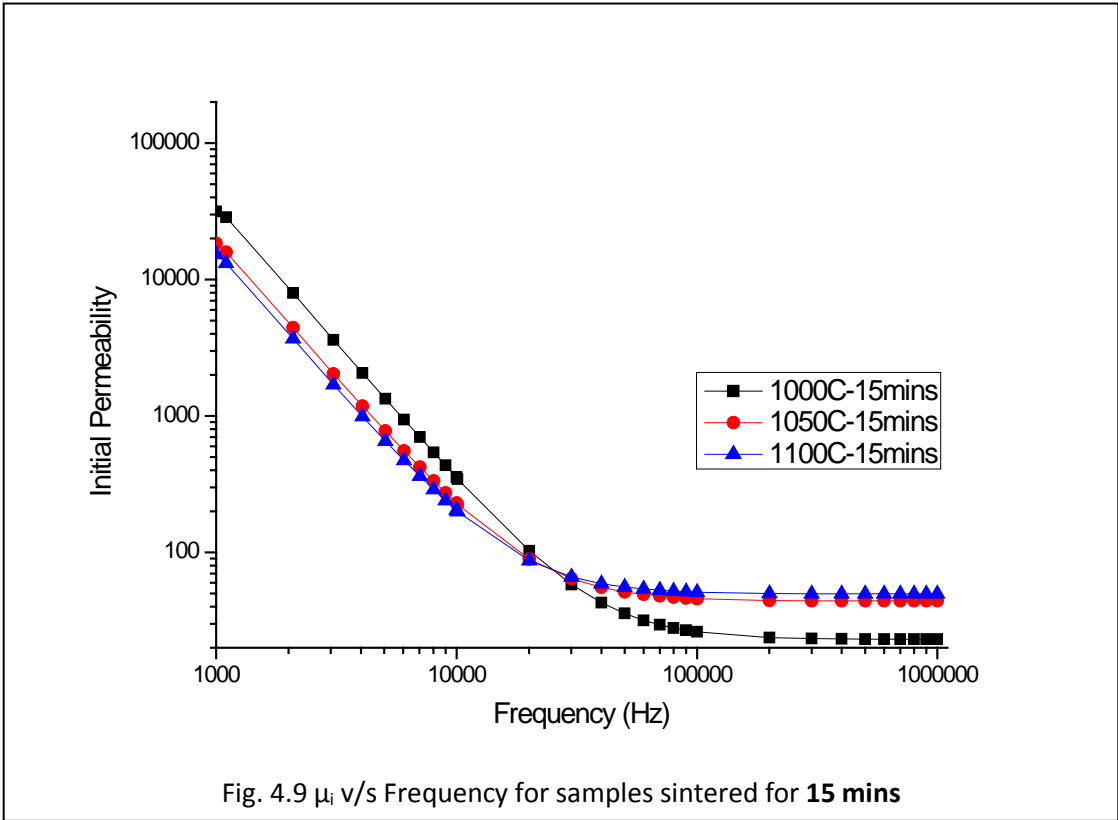
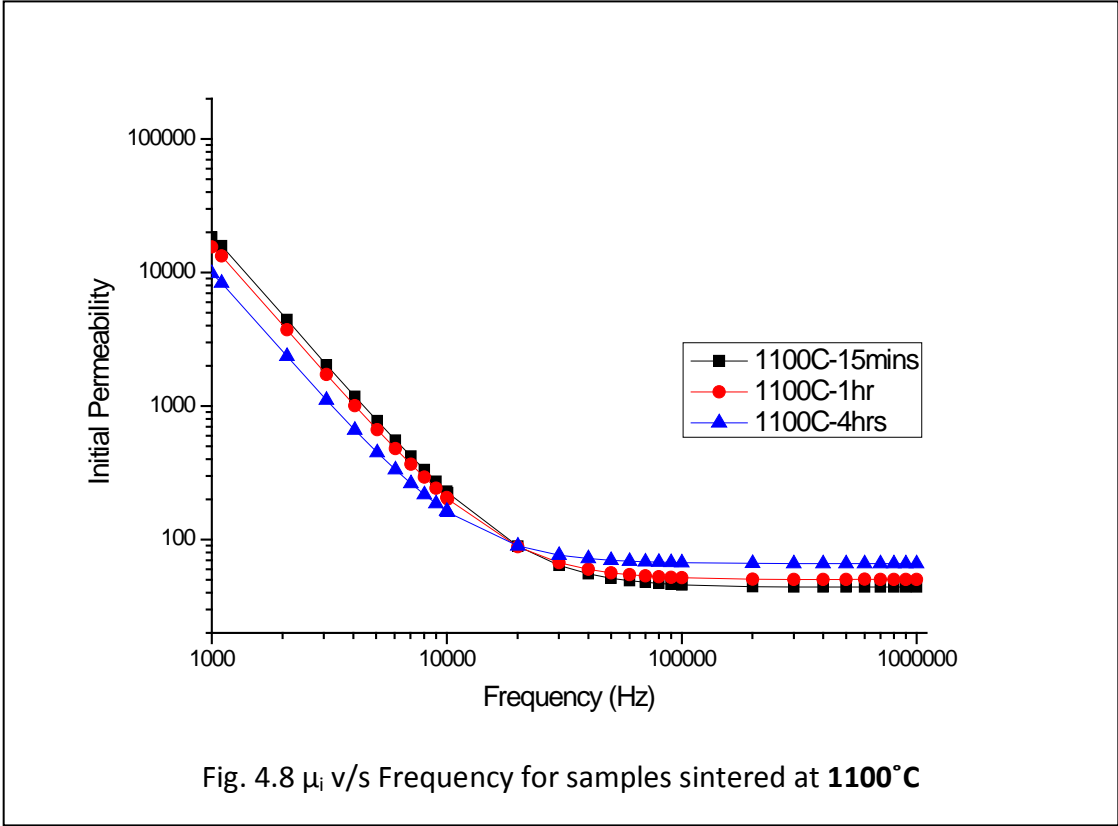
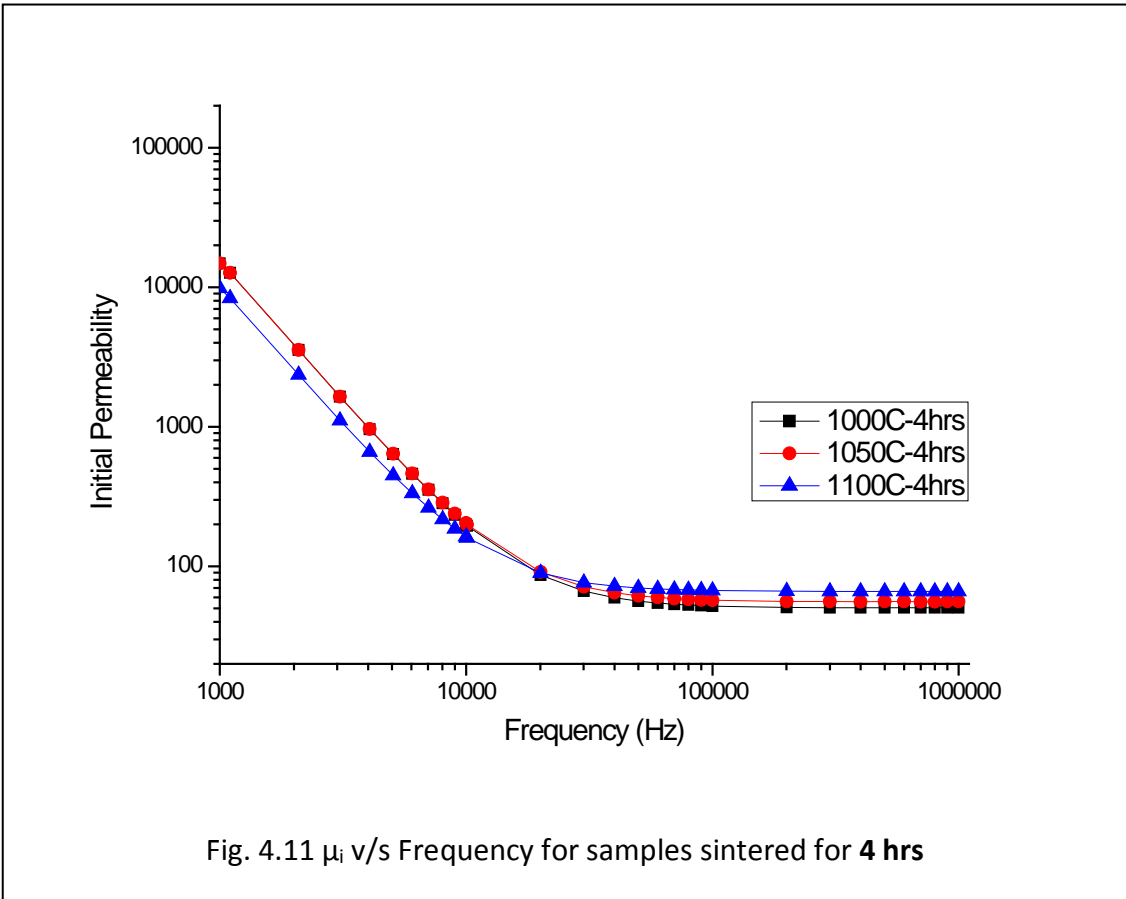
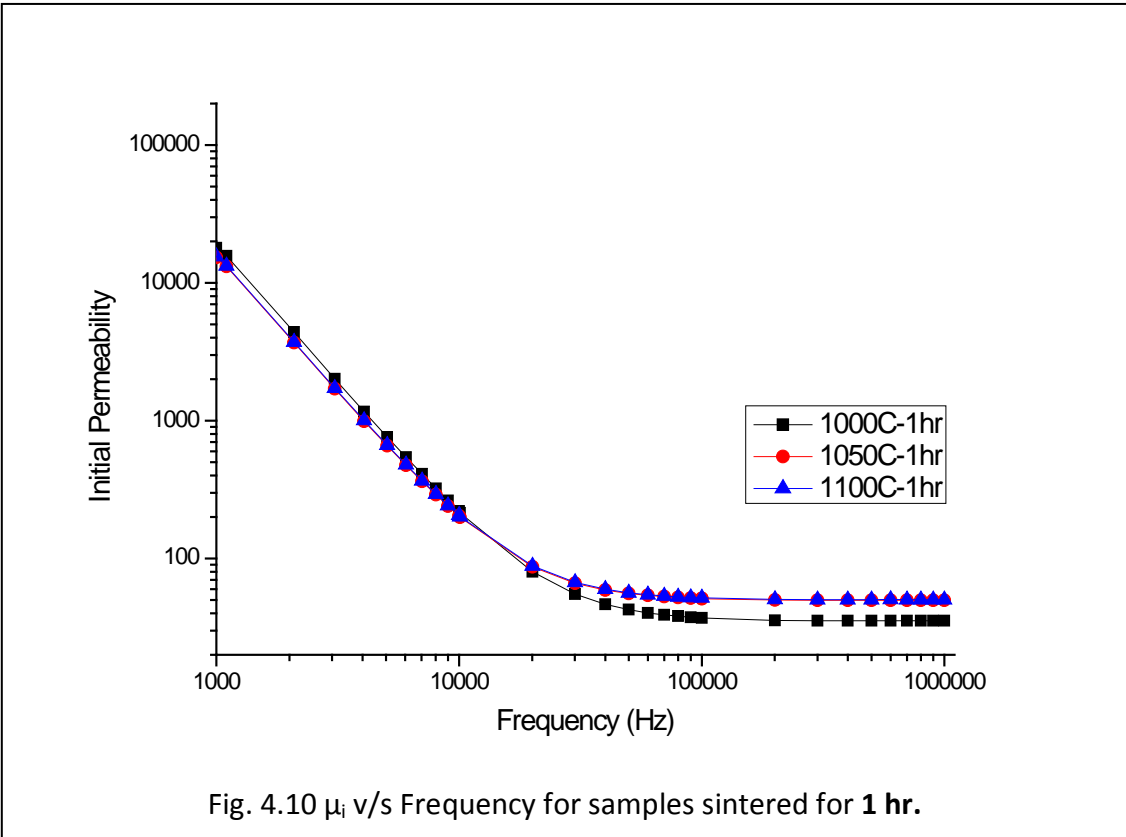


Fig 4. 6 to 4. 11 show the initial permeability vs frequency of the ferrite sintered at different temperatures and times. The initial permeability of a ferrite can be due to either a simultaneous rotation of the spin in each weiss-domain or to a reversible displacement or bulging of domain wall.





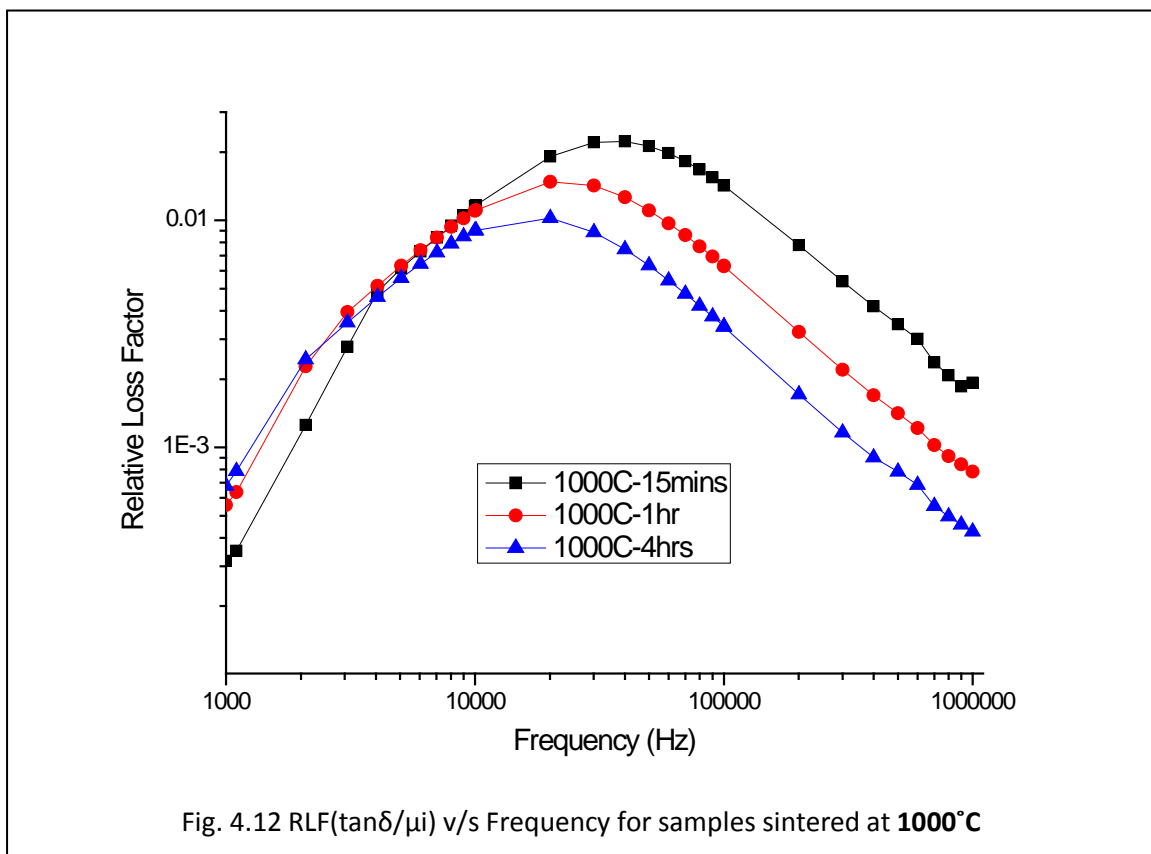


4.2.2 Loss

Losses in ferrites are due to 3 reasons:

- 1) Hysterisis loss: Mainly due to the non-reversing domain wall displacement.
- 2) Eddie-current loss: Due to the electronic movement to cancel the applied magnetic field. In most of the ferrites, eddie-current losses are negligible, but it is very high for metallic magnetic material.
- 3) Resonance relaxation losses: Due to either reversible high frequency displacement of domain wall or to the magnetization rotation inside a domain.

Fig 4. 12 to 4.17 show the relative loss factor ($\tan\delta/\mu_i$) vs frequency of the ferrites sintered at different temperatures and times.



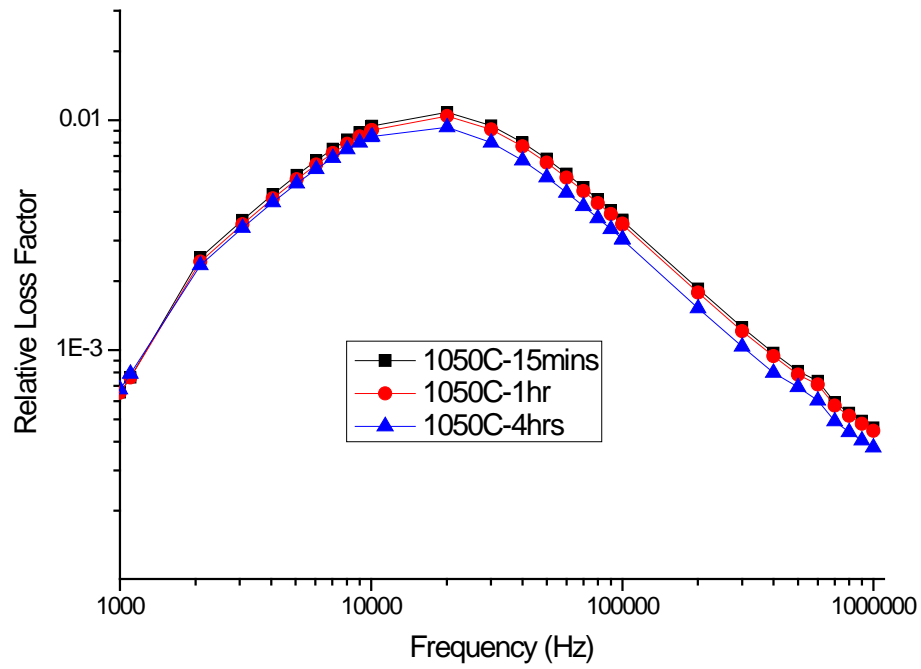


Fig. 4.13 RLF($\tan\delta/\mu$) v/s Frequency for samples sintered at **1050°C**

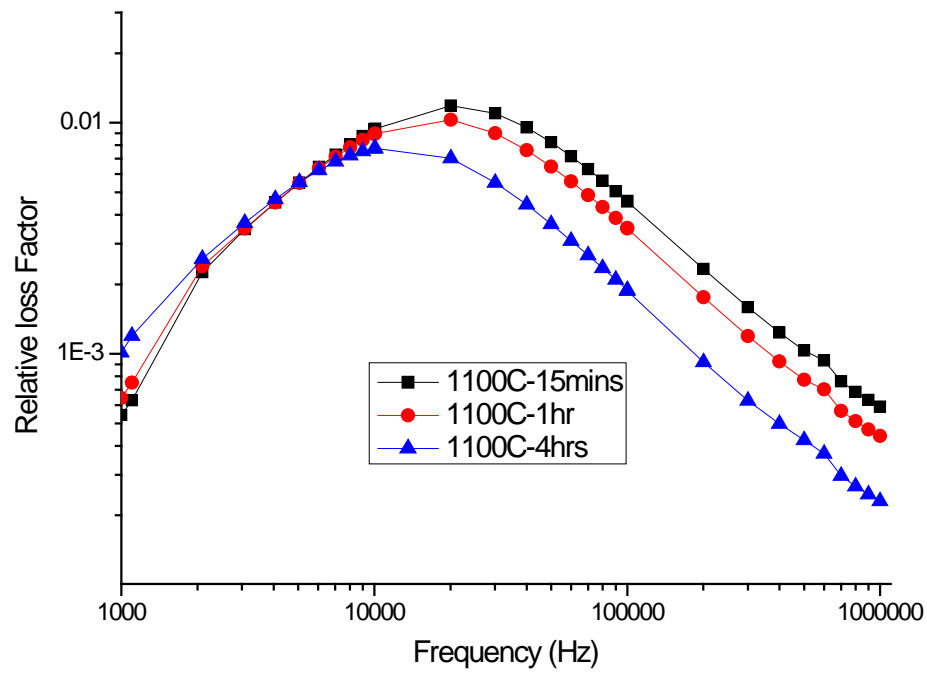


Fig. 4.14 RLF($\tan\delta/\mu$) v/s Frequency for samples sintered at **1100°C**

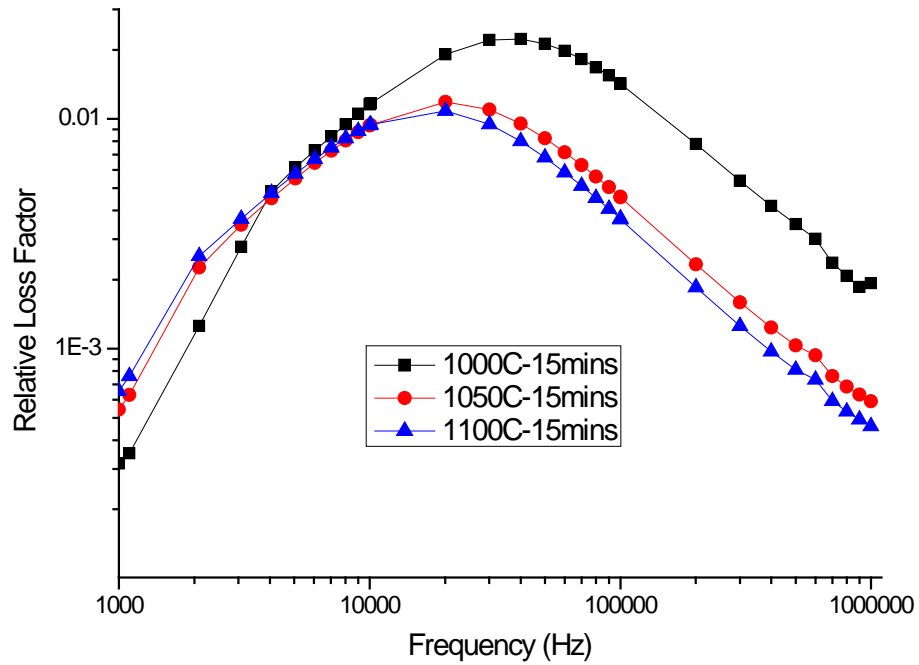


Fig. 4.15 RLF($\tan\delta/\mu_i$) v/s Frequency for samples sintered for **15 mins**

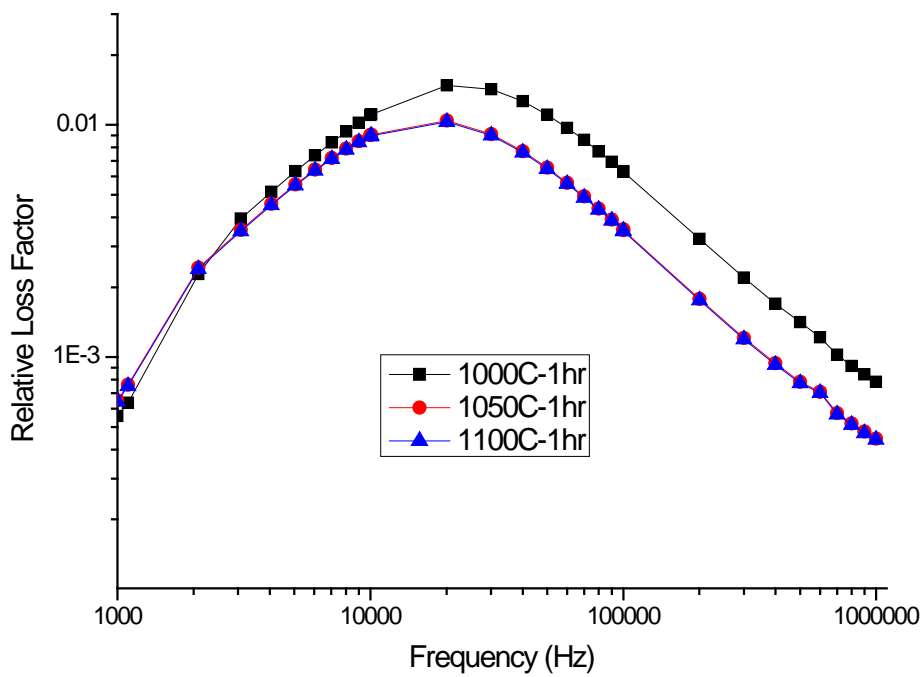
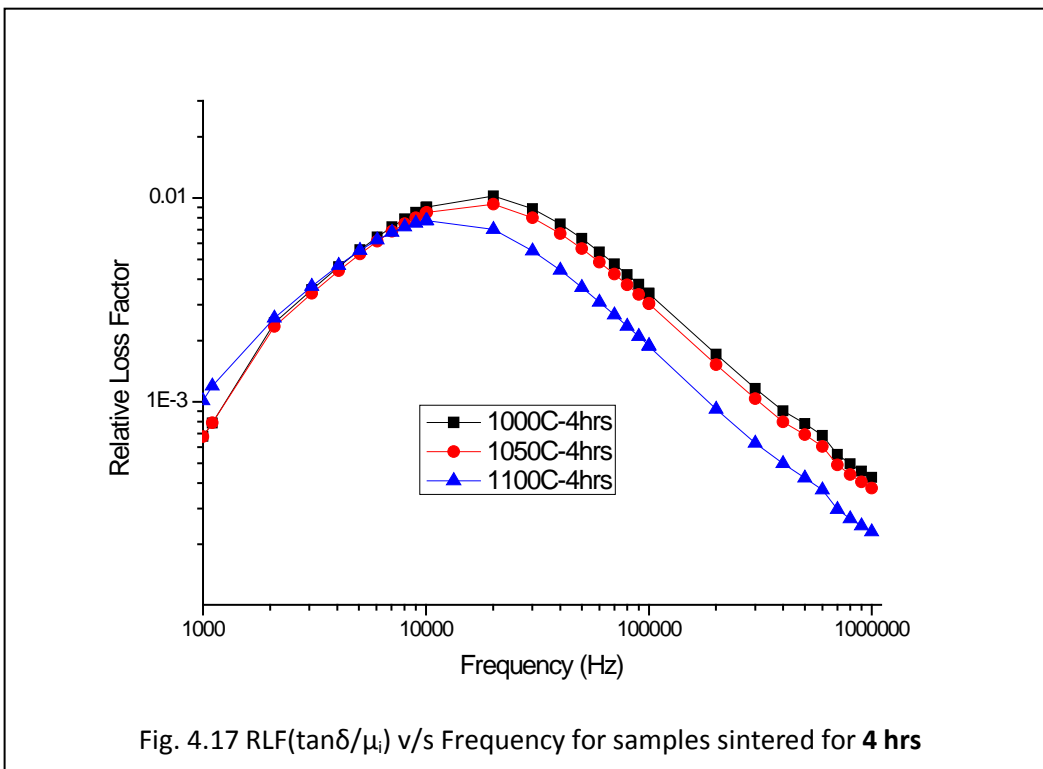
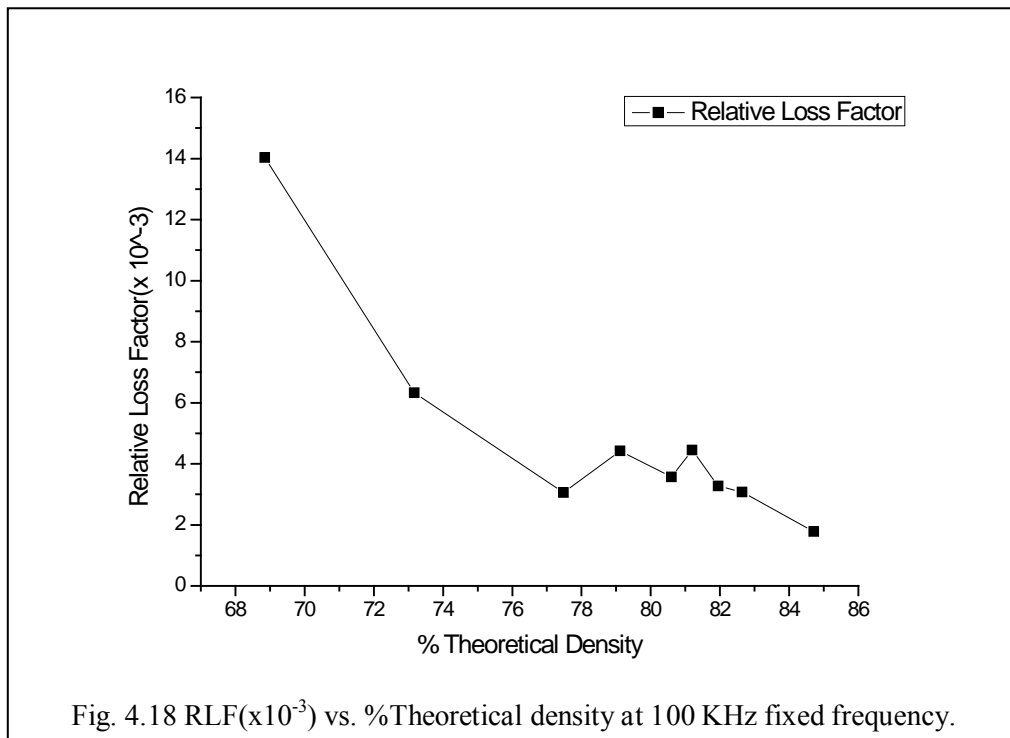


Fig. 4.16 RLF($\tan\delta/\mu_i$) v/s Frequency for samples sintered for **1 hr.**



Usually, hysteresis and eddie-current losses are predominant upto a frequency of 500 KHz. In the present case, loss is due to the hysteresis loss as eddie-current losses are negligible in the material at focus. Also it can be deduced from the study that losses decreased with increased densification (as shown in fig. 4.18).



CONCLUSIONS

NiZn ferrite sintered at different temperature and times showed that the permeability is highly dependent on density of the ferrite. Permeability increases with the increase in density. Relative loss was also found to depend on the relative density. Loss was lower for highly dense material.

References

1	Carter C. Barry, Norton M. Grant, Ceramic Materials Science and Engineering, Springer, 2007
2	Moulson A. J. and Herbert J. M., Electroceramics Materials Properties Applications, Wiley, 2003
3	Monica Sorescu, L. Diamandescu, R. Peelamedu, R. Roy, P. Yadoji, “Structural and magnetic properties of NiZn ferrites prepared by microwave sintering” 279 (2004) pp. 195-201
4	Purushotham Yadoji, Ramesh Peelamedu, Dinesh Agrawal and Rustum Roy, “Microwave sintering of Ni–Zn ferrites: comparison with conventional sintering” Materials Science and Engineering B. 98 (2003) pp. 269-278
5	R. V. Mangalaraja, S. Ananthakumar, P. Manohar, F. D. Gnanam and M. Awano, “Characterization of $Mn_{0.8}Zn_{0.2}Fe_2O_4$ synthesized by flash combustion technique” Materials Science and Engineering A. 367 (2004) pp. 301-305
6	R. V. Mangalaraja, S. Ananthakumar, P. Manohar and F. D. Gnanam, “Initial permeability studies of Ni–Zn ferrites prepared by flash combustion technique” Materials Science and Engineering A. 355 (2003) pp. 320–324.
7	N. Rezlescu, L. Sachelarie, E. Rezlescu, C-L. Sava and P. D. Popa, “Influence of PbO on microstructure and properties of a NiZn ferrite”, Ceramics International 29 (2003) pp. 107-111.
8	A. Verma, T. C. Goeland R. G. Mendiratta, “Frequency variation of initial permeability of NiZn ferrites prepared by the citrate precursor method” Journal of Magnetism and Magnetic Materials. 210 (2000) pp. 274-278
9	Hong-Wen Wang and Shong-Chung Kung, “Crystallization of nanosized Ni–Zn ferrite powders prepared by hydrothermal method”, Journal of Magnetism and Magnetic Materials. 270 (2004) pp. 230-236.
10	Kuo Hui Wu, Yin Chiung Chang and Gao Pying Wang, “Preparation of NiZn ferrite/SiO ₂ nanocomposite powders by sol–gel auto-combustion method” Journal of Magnetism and Magnetic Materials. 269 (2004) pp. 150-155